

University of Groningen

## Recent results from the decay studies of high-energy isoscalar giant resonances

Hunyadi, M.; van den Berg, A. M.; Blasi, N.; Csatlos, M.; Csige, L.; Davids, B.; Fujiwara, M.; Garg, U.; Gulyas, J.; Harakeh, M. N.

*Published in:*  
Acta Physica Polonica B

**IMPORTANT NOTE: You are advised to consult the publisher's version (publisher's PDF) if you wish to cite from it. Please check the document version below.**

*Document Version*  
Publisher's PDF, also known as Version of record

*Publication date:*  
2007

[Link to publication in University of Groningen/UMCG research database](#)

### *Citation for published version (APA):*

Hunyadi, M., van den Berg, A. M., Blasi, N., Csatlos, M., Csige, L., Davids, B., Fujiwara, M., Garg, U., Gulyas, J., Harakeh, M. N., de Huu, M. A., Krasznahorkay, A., Sohler, D., & Wortche, H. J. (2007). Recent results from the decay studies of high-energy isoscalar giant resonances. *Acta Physica Polonica B*, 38(4), 1479-1488.

### **Copyright**

Other than for strictly personal use, it is not permitted to download or to forward/distribute the text or part of it without the consent of the author(s) and/or copyright holder(s), unless the work is under an open content license (like Creative Commons).

The publication may also be distributed here under the terms of Article 25fa of the Dutch Copyright Act, indicated by the "Taverne" license. More information can be found on the University of Groningen website: <https://www.rug.nl/library/open-access/self-archiving-pure/taverne-amendment>.

### **Take-down policy**

If you believe that this document breaches copyright please contact us providing details, and we will remove access to the work immediately and investigate your claim.

*Downloaded from the University of Groningen/UMCG research database (Pure): <http://www.rug.nl/research/portal>. For technical reasons the number of authors shown on this cover page is limited to 10 maximum.*

RECENT RESULTS FROM THE DECAY STUDIES OF  
HIGH-ENERGY ISOSCALAR GIANT RESONANCES\*

M. HUNYADI<sup>a,b</sup>, A.M. VAN DEN BERG<sup>b</sup>, N. BLASI<sup>c</sup>, M. CSATLÓS<sup>a</sup>  
L. CSIGE<sup>a</sup>, B. DAVIDS<sup>b</sup>, M. FUJIWARA<sup>d</sup>, U. GARG<sup>e</sup>, J. GULYÁS<sup>a</sup>  
M.N. HARAKEH<sup>b</sup>, M.A. DE HUU<sup>b</sup>, A. KRASZNAHORKAY<sup>a</sup>  
D. SOHLER<sup>a</sup>, H.J. WÖRTCHE<sup>b</sup>

<sup>a</sup>Institute of Nuclear Research, Hungarian Academy of Sciences  
Debrecen, Hungary

<sup>b</sup>Kernfysisch Versneller Instituut, Groningen, The Netherlands

<sup>c</sup>Istituto Nazionale di Fisica Nucleare — Sezione di Milano, Italy

<sup>d</sup>Research Center for Nuclear Physics (RCNP), Osaka, Japan

<sup>e</sup>University of Notre Dame, Notre Dame, USA

*(Received November 11, 2006)*

The direct and statistical neutron decay of the isoscalar giant dipole resonance and a continuum region at higher excitation energy has been studied in  $^{90}\text{Zr}$ ,  $^{116}\text{Sn}$  and  $^{208}\text{Pb}$  using the  $(\alpha, \alpha'n)$  reaction at a bombarding energy of 200 MeV. The spectra of fast decay neutrons populating valence neutron-hole states were analyzed, and estimates for the branching ratios were determined to compare to recent theoretical predictions. The observation of the direct nucleon decay channels helped to separate giant resonance strengths and suppress the underlying background and continuum, which lead to an indication for the existence of the first overtone mode of the isoscalar giant quadrupole resonance.

PACS numbers: 24.30.Cz, 25.55.Ci, 27.60.+j, 27.80.+w

## 1. Introduction

The experimental investigations of direct decay modes of giant resonances are of special importance for a better understanding of how the microscopic structure of nuclei evolves to collective behavior. Since most of the giant resonances are located above the particle separation thresholds, particle emission is the dominant decay process that can take place at different stages of the damping process [1]. The particle decay can occur either from

---

\* Presented at the Zakopane Conference on Nuclear Physics, September 4–10, 2006, Zakopane, Poland.

the initial  $1p-1h$  state leaving a single-hole state in the  $A - 1$  nucleus (direct decay), or from the states with partially or completely equilibrated configurations, resulting in an evaporation-like spectrum of the emitted particles (statistical decay). The observation of particle emission spectra following the excitation of giant resonances and the determination of the branching ratios thus provide information on the evolution of the decaying configuration and on the microscopic structure of the giant resonance.

Beside the main interest of studying isoscalar giant resonances in particle-decay experiments a systematic investigation of compression modes (ISGMR, ISGDR) was pursued in connection with the experimental determination of the nuclear incompressibility due to its direct relationship with the excitation energy of these resonances [2–5]. Singles experiments ([6–15]) using inelastic  $\alpha$ -scattering were devoted to deduce more precise values of the incompressibility, which has a crucial role in the application of the nuclear equation-of-state, *e.g.* in model calculations of various astrophysical processes or in descriptions of heavy-ion reactions. These experiments focused on the detailed investigations of the ISGMR in the last two decades following its discovery in 1977 [16, 17], while the first unambiguous evidence for the existence of the ISGDR was reported only in 1997 [10]. The difficulties were mainly caused by the relatively weak excitation of the  $3\hbar\omega$  ISGDR, which in addition was distributed with a relatively large width superimposed upon an overwhelming nuclear continuum and instrumental background. Moreover, a partial overlap with the  $3\hbar\omega$  high-energy octupole resonance (HEOR) further increased the uncertainties of the resonance parameters. Consequently, very little is known about the ISGDR and its microscopic structure. The only experimental result on its proton-decay properties in  $^{208}\text{Pb}$  was first reported in Ref. [18].

In the last few years, experimental studies aimed at drawing a consistent picture of the ISGDR systematics using multipole-decomposition analysis (MDA). However, the problem of separating the nuclear-background components from resonance strengths still remained due to the unknown multipole contents of the nuclear continuum [11–15]. This MDA technique requires high-precision measurements in a wide angular region to decompose the spectra confidently, however, the results strongly depend on the model assumptions. Alternatively, the pronounced changes and large differences in the shapes of the angular distributions at very forward angles can also be exploited, and various multipolarities (especially  $L \leq 2$ ) can easily be disentangled in a less model-dependent way [10, 19, 20]. These measurements close to  $0^\circ$  often suffered from a substantial contribution of instrumental background in addition to the nuclear continuum of non-resonant processes of quasi-free scattering and various pick-up/break-up reactions. The elimination of the background components was the major difficulty in the sin-

gles experiments, and the hypothetical choice of the background-subtraction technique resulted in large uncertainties which added to the statistical error of giant-resonance parameters.

Beside the main experimental goal of our decay measurements on studying direct-decay properties and microscopic structure of the ISGDR, it was important to overcome the problems connected with the background subtraction. Placing the coincidence detectors at backward angles the nuclear continuum is expected to be suppressed, which filters out events associated with forward-peaked processes like quasi-free scattering and pick-up/break-up reactions. Furthermore, by gating on the particle direct-decay channels, contributions from excitation of more complex ( $np$ - $nh$ ) states are removed, and the direct decay from initial  $1p$ - $1h$  configurations is enhanced.

We report a description of our coincidence experiments for studying the direct neutron-decay properties of the ISGDR in  $^{90}\text{Zr}$ ,  $^{116}\text{Sn}$  and  $^{208}\text{Pb}$ . We also planned to focus on resonances in the continuum region above the ISGDR, where overtone modes of the ISGQR and ISGMR are predicted by continuum-RPA calculations [21]. This was primarily motivated by experimental indications reported in the previous work on direct proton-decay measurements [22], and by the intensive efforts of continuum-RPA calculations to describe the main properties of such high-energy resonance modes.

## 2. Experiment

The experiments were performed at the AGOR superconducting cyclotron facility at KVI, which provided an  $\alpha$ -particle beam with energy of 200 MeV on  $^{90}\text{Zr}$ ,  $^{116}\text{Sn}$  and  $^{208}\text{Pb}$  targets. The ejectiles were momentum analyzed by the Big-Bite Spectrometer (BBS) [23], which is equipped with a composite focal-plane detector system [24]. The decay neutrons were observed in coincidence with the ejectiles with the large-coverage detector array (EDEN) [25] placed in the backward hemisphere with respect to the beam direction. In the present setup the neutron-detector array consisted of 30 organic-liquid scintillators of type NE213 built for precise time-of-flight (TOF) measurements at a distance of 1.6 m from the target position. In this arrangement the 30 detectors covered a solid angle of 2.9% of  $4\pi$ .

Various sources of the background events in the neutron detectors had to be identified and suppressed in order to reduce the statistical error of the TOF-measurement. On the other hand, the high flux of  $\gamma$ -rays from the target was identified and separated exploiting the pulse-shape discrimination (PSD) capability of this scintillator material, which is based on the different decay times of light signals induced by particles with different ionization mechanisms in the scintillator material.

An overall time resolution of 1.8 ns was determined for the prompt  $\gamma$ -peak, which corresponded to an energy resolution of 1.5–2 MeV for fast neutrons with a kinetic energy in the range of interest ( $E_n=12$ -16 MeV).

The combination of the BBS and the ESN focal-plane detector was an effective and well-suited tool to satisfy the requirements for particle-identification, momentum analysis and the reconstruction of scattering angle of the ejectiles. The ESN detector was designed to measure the incident positions and angles of scattered particles by two 2-dimensional vertical-drift chambers (VDC) in the focal plane, which allowed the observation of an excitation-energy range of 10–70 MeV due to the large momentum acceptance of the spectrometer.

An energy resolution of  $\sim 350$  keV was determined with measurements on a  $^{12}\text{C}$  target. However, this resolution in combination with that of the decay neutrons in the direct-decay channels exceeded the average level distance at low excitation energies in the daughter nuclei, which was obviously insufficient to resolve the individual neutron-hole states. Nevertheless, a good separation of the direct- and statistical-decay components was still possible, and integrated branching ratios for the direct-decay components could be deduced.

### 3. Experimental results

Singles spectra of inelastic  $\alpha$ -scattering were measured simultaneously with the coincidence spectra to obtain differential cross sections of the ISGDR for the determination of the branching ratios and exhaustion factors of the EWSR. In general, multipole strengths in inelastic-scattering spectra of inclusive measurements are evaluated with the multipole decomposition analysis (MDA), provided a sufficiently wide angular region is measured. However, the MDA can effectively be employed for strongly excited resonance structures (*e.g.* ISGQR, ISGMR), where the relative contribution of the background is small, while weak resonances at higher excitation energies can only be analyzed with large statistical uncertainties and the resonance strengths cannot be separated from the continuum for a given multipolarity. This can mainly be the consequence of the assumption that several multipolarities are present in the nuclear continuum, and components of higher angular momenta ( $L \geq 3$ ) possessing similar angular distributions at the forward scattering angles are less confidently decomposed. In the alternative technique of the difference-of-spectra (DOS), this feature of angular distributions is exploited to separate multipolarities of high and low angular momenta. The angular acceptance of the spectrometer in the present experiments ( $1.5^\circ$ – $5.5^\circ$ ) covered a region, in which the differential cross section for  $L = 1$  has both a maximum and a local minimum. Contributions of

multipole strengths, especially of the HEOR, overlapping in excitation energy with ISGDR had to be minimized by the appropriate choice of angular regions in the DOS procedure. The  $(\alpha, \alpha')$ -spectra were generated at these angles and subtracted as shown in Fig. 1. The enhancement of the  $L = 1$  component is significant in the difference spectra around the excitation energies of the ISGDR.

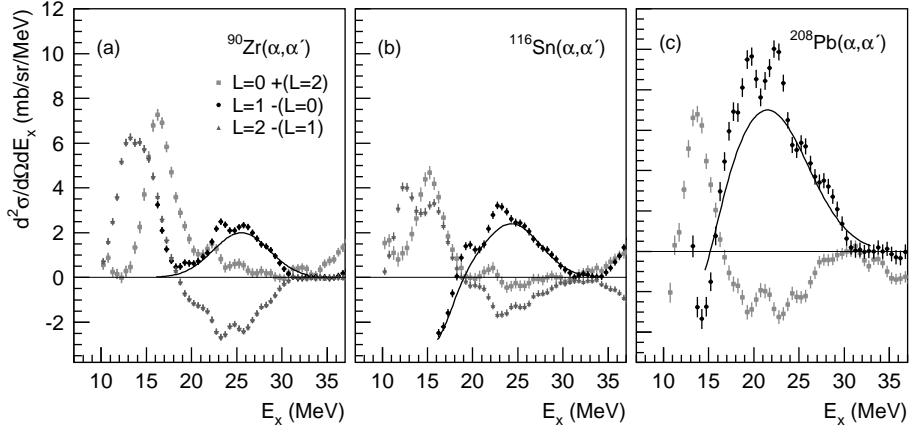


Fig. 1. Difference spectra in terms of double-differential cross sections from the singles measurements. The plots represent difference spectra selecting multipolarities with  $L = 0, 1,$  and  $2$ . Contributions of other multipolarities are given in brackets, which could not be eliminated by the difference-of-spectra procedure in the observed angular region. The curves represent the cross section for the  $(\alpha, \alpha')$  reaction composed of Gaussians for the ISGDR and the ISGMR (with opposite signs), excluding the superimposed structures due to the contaminant  $^{16}\text{O}(\alpha, \alpha')$  reaction.

At excitation energies above the ISGDR region some  $L = 1$  strength is still present, which can be attributed to the  $L = 1$  component of the nuclear continuum excited through quasi-free processes. The low-energy tail of this continuum distribution was estimated by smooth curves (dashed curves in Fig. 1) extrapolating in the ISGDR region. Further appearance of  $L = 0$  and  $L = 2$  strengths in the  $3\hbar\omega$  region is not expected, nevertheless small contributions of  $L = 0$  and  $L = 2$   $4\hbar\omega$  overtones to the ISGDR cannot be excluded as they are predicted to have relatively large widths due to their stronger damping and less concentrated particle-hole states.

The differential cross sections for the ISGDR regions were obtained by the integration of the double-differential cross sections in the  $L = 1$  difference spectra excluding contributions of quasi-free continuum and reactions on oxygen contamination of the target. The results are listed in Table I and compared to the theoretical values from DWBA calculation.

TABLE I

Differential cross sections and direct neutron-decay branching ratios (Br) obtained from the analysis of singles and coincidence data for the  $L = 1$  strength in the ISGDR region. The experimental and theoretical differential cross sections of giant-resonance structures identified in the singles DOS were compared. The theoretical values were calculated in DWBA assuming 100% exhaustion of the respective EWSR. The differential cross sections for the ISGDR in the direct-decay channel were determined by a simplified MDA (see in the text). Branching ratios (Br) for the total direct-decay components were determined and compared to the results of continuum-RPA calculations summed for the decay channels populating the valence single-hole states.

Nucleus	Singles data $d\sigma/d\Omega$ (mb/sr)	Direct-decay $d\sigma/d\Omega$ (mb/sr)	This work Br (%)	Theory [21] Br (%)
$^{90}\text{Zr}$	16.5(2.0)	0.80(0.10)	4.8(0.9)	16.8
$^{116}\text{Sn}$	20.7(1.5)	1.05(0.12)	5.1(0.7)	10.85
$^{208}\text{Pb}$	38.0(5.0)	3.99(0.31)	10.5(1.6)	11.46

As a first step of analyzing the coincidence data, various background components due to the instrumentally induced events and quasi-free knock-out processes were eliminated in the spectra by correcting for random coincidences and by measuring the neutrons at backward angles, respectively. The background remaining in the coincidence spectra must be associated with inelastic scattering into the nuclear continuum. The discrimination between this continuum and the resonance strengths exploits the principal differences in their decay properties and their angular distributions. States of complex  $np$ - $nh$  excitations can also decay by particle emission, which follows the statistical rules of particle evaporation.

The final-state spectra were generated for a region, where most of the ISGDR strength is known from previous singles experiments to be concentrated, and for the continuum at higher excitation energies. The results are shown in Fig. 2, in which the kinetic energy is converted to excitation energy of the daughter nucleus (final-state energy  $E_{f.s.}$ ). The spectra were compared to those of statistical decay calculations performed with the code CASCADE [26, 27], which are also plotted in Fig. 2. The steep shoulder of the statistical component was well reproduced by the calculation using a normalization to fit the experimental points.

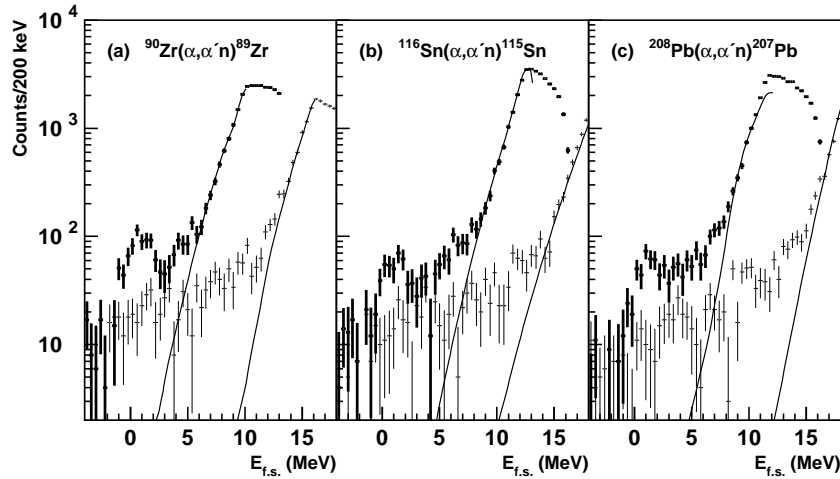


Fig. 2. Final-state spectra projected for events in the excitation energy region of the ISGDR (thick crosses) and of the continuum above (thin crosses). Statistical-decay calculations are represented by solid curves normalized to the experimental points. The excitation energy regions of the ISGDR and continuum were chosen to be 23–28 MeV ( $^{90}\text{Zr}$ ), 22–27 MeV ( $^{116}\text{Sn}$ ), 20–25 MeV ( $^{208}\text{Pb}$ ) and 30–36 MeV ( $^{90}\text{Zr}$ ), 29–35 MeV ( $^{116}\text{Sn}$ ), 27–32 MeV ( $^{208}\text{Pb}$ ), respectively.

The direct population of single-hole states from the ISGDR region appeared as prominent structures in all the three nuclei, clearly separated from the statistical components. However, the energy resolution of  $\sim 1500$  keV, stemming from the TOF measurement of faster neutrons, was insufficient to resolve the individual low-lying neutron-hole states and to extract partial branching ratios. It is worth noting that the population of single-hole states from decay of the ISGDR region is still more pronounced compared to that of the continuum at higher excitation energy. For the ISGDR region the semi-direct population of more complex final states in the energy range  $E_{f.s.} = 3\text{--}6$  MeV was not so visible as that of the single-hole states, but for the continuum region a rather smooth distribution was observed from the sharply rising edge of statistical decay to the lowest hole-states. The remarkable feature of the continuum is that a significant part of its decay could be attributed to non-statistical decay, which may suggest the presence of other resonance strengths at excitation energies above the ISGDR. These could most likely be attributed to modes with higher multiplicities and/or overtone resonances predicted in this region.

The part of the direct-decay population associated with  $L = 1$  strength in the ISGDR region was determined on basis of the analysis of angular distributions. It is assumed that from such a high excitation energy region only giant resonances decay to low-lying valence-hole states, therefore only



$L = 3$  multipolarity of the HEOR must be disentangled from the ISGDR. Following a simplified procedure of MDA with only  $L = 1$  and  $L = 3$  components, differential cross sections and branching ratios can be more accurately extracted than those from the DOS analysis.

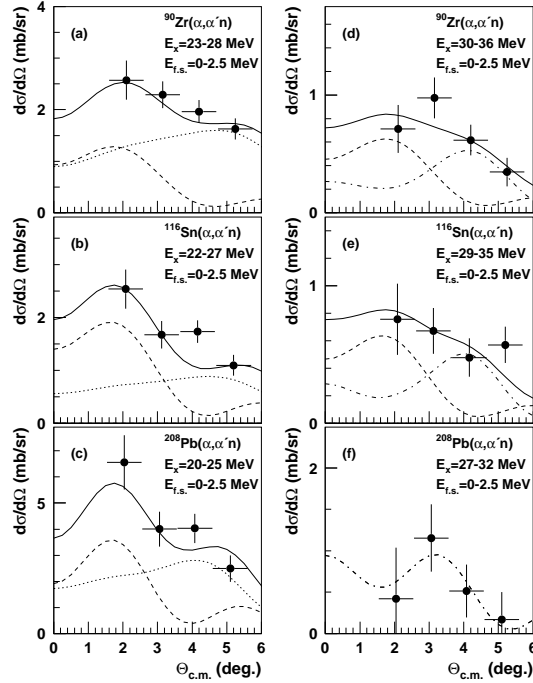


Fig. 3. Angular distributions in terms of differential cross sections for the ISGDR (left panels) and continuum (right panels) regions. The experimental points were fitted with angular distributions of the DWBA calculations for multiplicities, which are expected to be present in the given excitation energy regions:  $L = 1$  (dashed) and  $L = 3$  (dotted) for the ISGDR region;  $L = 1$  (dashed) and  $L = 2$  (dashed-dotted) for the continuum region.

The continuum region above the ISGDR was also analyzed by this fitting procedure assuming the presence of strengths with  $L = 0, 1$  and  $2$ . The results are shown in Fig. 3 selecting the pronounced bump of the low-lying states in the final-state spectra below  $E_{f.s.}=2.5$  MeV. It was found that the direct-decay of the continuum region in  $^{90}\text{Zr}$  and  $^{116}\text{Sn}$  can be associated with a mixed multipole strengths of  $L = 1$  and  $2$ , but for  $^{208}\text{Pb}$  the best fit was obtained for a pure  $L = 2$  distribution. This observation is confirmed by the result of our previous experiment on the direct proton-decay studies [22], where a significant enhancement of  $L = 2$  double-differential cross section was found centering at  $E_x=26.9\pm 0.7$  MeV. Based on the continuum-RPA

calculation of Ref. [21], which predicts the overtone mode of the ISGQR in  $^{208}\text{Pb}$  at  $E_x=30.5$  MeV, the present observation of the  $L = 2$  strength in this excitation energy region may be assigned to this resonance mode.

The branching ratios determined for the direct decay from the  $L = 1$  strength of the ISGDR region are listed in Table I and compared to the results of the continuum-RPA calculations from Ref. [21]. Since the single-hole states could not be resolved due to the insufficient energy resolution, the theoretical partial branching ratios had to be summed up for the valence neutron-hole states to compare with the experimental values.

As a result, the experimental branching ratios of the ISGDR showed an excellent agreement for  $^{208}\text{Pb}$ , while those for  $^{90}\text{Zr}$  and  $^{116}\text{Sn}$  were found significantly lower than predicted theoretically. In the case of  $^{116}\text{Sn}$ , the deviation of a factor of  $\approx 2$  can partly be explained by an overestimation of the calculations, since experimental values of the spectroscopic factors for the single-hole states in question are typically 50–60% of the single-particle limit. In the case of  $^{90}\text{Zr}$ , this argument cannot account for the large deficiency of single-hole-state population in the experiment, where a factor of 3.5 was found with respect to the calculations. This disagreement cannot be explained on the basis of the present theoretical descriptions.

#### 4. Conclusions

In summary, we have investigated the direct neutron-decay channels of the ISGDR in  $^{90}\text{Zr}$ ,  $^{116}\text{Sn}$  and  $^{208}\text{Pb}$  by observing the population of low-lying, single neutron-hole states in the respective daughter nuclei. The decay properties of the ISGDR and a continuum region above the ISGDR were studied, and direct-decay branching ratios were determined. The decay of the ISGDR region showed an increased population of the single-hole states compared to the decay of the continuum region, however, the presence of resonance strengths at higher excitation energies could not be excluded. On the other hand, the analysis of angular distributions for the continuum region associated with the decay to low-lying states indicated the presence of  $L = 2$  strengths. In the case of  $^{208}\text{Pb}$ , this may be associated with the overtone of the ISGQR, however weak indications for its presence were also found in  $^{90}\text{Zr}$  and  $^{116}\text{Sn}$ .

We acknowledge the European Commission support in the frameworks of the Marie Curie Fellowship and Reintegration programs under contract HPMF-CT-2000-00663 and MERG-CT-2004-006379, and transnational access program under contract HPRI-CT-1999-00109, and the Hungarian Fund OTKA under contracts N32570, D34587 and NK69035. This work was performed as part of the research program of the Dutch Stichting voor Fun-

damenteel Onderzoek der Materie (FOM) with financial support from the Nederlandse Organisatie voor Wetenschappelijk Onderzoek (NWO). U. Garg acknowledges a grant from the U.S. National Science Foundation (number PHY-0140324). M. Hunyadi acknowledges a grant from the János Bolyai Research Fellowship of the Hungarian Academy of Sciences.

## REFERENCES

- [1] M.N. Harakeh, A. van der Woude, *Giant Resonances: Fundamental High-Frequency Modes of Nuclear Excitations*, Oxford University Press, New York 2001, and reference therein.
- [2] M.N. Harakeh, A.E.L. Dieperink, *Phys. Rev.* **C23**, 2329 (1981).
- [3] S. Stringari, *Phys. Lett.* **B108**, 232 (1982).
- [4] G. Colò, *Phys. Lett.* **B485**, 362 (2000).
- [5] S. Shlomo, A.I. Sanzhur, *Phys. Rev.* **C65**, 044310 (2002).
- [6] C. Djalali *et al.*, *Nucl. Phys.* **A380**, 42 (1982).
- [7] H.P. Morsch *et al.*, *Phys. Rev. Lett.* **45**, 337 (1980).
- [8] H.P. Morsch *et al.*, *Phys. Rev.* **C28**, 1947 (1983).
- [9] G.S. Adams *et al.*, *Phys. Rev.* **C33**, 2054 (1986).
- [10] B.F. Davis *et al.*, *Phys. Rev. Lett.* **79**, 609 (1997).
- [11] H.L. Clark *et al.*, *Phys. Rev.* **C63**, 031301 (2001).
- [12] M. Uchida *et al.*, *Phys. Lett.* **B557**, 12 (2003).
- [13] Y.-W. Lui *et al.*, *Nucl. Phys.* **A731**, 28c (2004).
- [14] D.H. Youngblood *et al.*, *Phys. Rev.* **C69**, 054312 (2004a).
- [15] D.H. Youngblood *et al.*, *Phys. Rev.* **C69**, 034315 (2004b).
- [16] M.N. Harakeh *et al.*, *Phys. Rev. Lett.* **38**, 676 (1977).
- [17] D.H. Youngblood *et al.*, *Phys. Rev. Lett.* **39**, 1188 (1977).
- [18] M. Hunyadi *et al.*, *Nucl. Phys.* **A731**, 49c (2004).
- [19] S. Brandenburg *et al.*, *Nucl. Phys.* **A466**, 29 (1987).
- [20] S. Brandenburg *et al.*, *Phys. Rev.* **C39**, 2448 (1989).
- [21] M.L. Gorelik *et al.*, *Phys. Rev.* **C69**, 054322 (2004).
- [22] M. Hunyadi *et al.*, *Phys. Lett.* **B576**, 253 (2003).
- [23] A.M. van den Berg, *Nucl. Instrum. Methods* **B99**, 637 (1995).
- [24] H.J. Wörtche, *Nucl. Phys.* **A687**, 321c (2001).
- [25] H. Laurent *et al.*, *Nucl. Instrum. Methods* **A326**, 517 (1993).
- [26] F. Pühlhofer, *Nucl. Phys.* **A280**, 267 (1977).
- [27] M.N. Harakeh, Program CASCADE, extended version (1983).